© 2021. Published by The Company of Biologists Ltd | Journal of Experimental Biology (2021) 224, jeb233965. doi:10.1242/jeb.233965

RESEARCH ARTICLE

The high energetic cost of rapid force development in muscle

Tim J. van der Zee* and Arthur D. Kuo

ABSTRACT

Muscles consume metabolic energy for active movement, particularly when performing mechanical work or producing force. Less appreciated is the cost for activating muscle quickly, which adds considerably to the overall cost of cyclic force production. However, the cost magnitude relative to the cost of mechanical work, which features in many movements, is unknown. We therefore tested whether fast activation is costly compared with performing work or producing isometric force. We hypothesized that metabolic cost would increase with a proposed measure termed force rate (rate of increase in muscle force) in cyclic tasks, separate from mechanical work or average force level. We tested humans (N=9) producing cyclic knee extension torque against an isometric dynamometer (torque 22 N m, cyclic waveform frequencies 0.5–2.5 Hz), while also quantifying quadriceps muscle force and work against series elasticity (with ultrasonography), along with metabolic rate through respirometry. Net metabolic rate increased by more than four-fold (10.5 to 46.8 W) with waveform frequency. At high frequencies, the hypothesized force-rate cost accounted for nearly half (40%) of energy expenditure. This exceeded the cost for average force (17%) and was comparable to the cost for shortening work (43%). The force-rate cost is explained by additional active calcium transport necessary for producing forces at increasing waveform frequencies, owing to rate-limiting dynamics of force production. The force-rate cost could contribute substantially to the overall cost of movements that require cyclic muscle activation, such as locomotion.

KEY WORDS: Metabolic energy, Muscle activation, Isometric force, Biomechanics, Calcium transport

INTRODUCTION

Humans often expend energy to perform movement tasks where muscles are only intermittently or cyclically active. Two notable contributions to the metabolic cost of such tasks are for the mechanical work performed by muscle fascicles (Abbott et al., 1952; Margaria, 1968), and for the force exerted when fascicles are isometric (Crow and Kushmerick, 1982). Less appreciated is the cost for muscle activation during intermittent or cyclic conditions. This cost increases with briefer contractions (Hogan et al., 1998) or higher rates of force production (Doke and Kuo, 2007), and can exceed the cost for producing continuous isometric force (Chasiotis et al., 1987). However, there is also substantial metabolic energy expended in tasks that also entail work; for example, locomotion with the lower extremity (Margaria, 1976) or reaching with the upper extremity (Huang et al., 2012). But the relative cost for activating muscle versus performing work in such tasks remains unknown. It is therefore helpful to determine whether the cost for activating muscle is comparable to the cost for work and force production.

There is clearly an energetic cost for activating muscle under intermittent, isometric conditions. This has been demonstrated with square-wave, on–off activation patterns, which yield a considerably higher metabolic cost than continuous activation at similar overall contraction duration (Chasiotis et al., 1987; Spriet et al., 1988). Intermittent contraction also requires more metabolic energy when contraction frequency is higher (Bergström and Hultman, 1988; Hogan et al., 1998) or when duration of active force production is shorter (Beck et al., 2020), even when accounting for the cost of maintaining isometric force, which is roughly proportional to the force–time integral (Crow and Kushmerick, 1982). For example, metabolic cost increases with the frequency of muscle activation (Bergström and Hultman, 1988), leading to a doubling of energetic cost per unit force compared to continuous isometric force (Chasiotis et al., 1987). The underlying mechanism is thought not to be related to crossbridge work, as the activation cost has been attributed to active calcium transport (Hogan et al., 1998).

There is also a similar metabolic cost for cyclic, non-isometric movements. For example, cyclic leg swinging (Doke et al., 2005; Doke and Kuo, 2007) and ankle bouncing (Dean and Kuo, 2011) have costs increasing markedly with movement frequency (e.g. three- to four-fold for a 45% increase in frequency; Doke et al., 2005). The costs are not explained by the amount of mechanical work, and have also been associated with calcium transport (Doke and Kuo, 2007). For cyclic movements, the cost has been related to the rate of force production, or force rate, which may be considered an analogue of on–off intermittency, but for continuous, non-isometric movements. The cost of leg swinging, including a force-rate component, could account for one-third of the net metabolic cost of walking (Doke et al., 2005). The hypothesized force-rate cost may therefore be relevant to typical human activities.

However, it remains unclear to what extent the force-rate cost contributes to overall metabolic cost of movement. Everyday movements may have substantial costs for work and force production. This makes it difficult to separate the force-rate cost and quantify its contribution relative to other costs. The force-rate cost seems to be present when muscle–tendon complex work is controlled for (e.g. Chasiotis et al., 1987; Doke and Kuo, 2007). However, muscle fascicles can perform work on series elasticity, not observable from the overall muscle–tendon complex. Even in apparently isometric conditions, such work may contribute substantially to overall cost. After all, muscle fascicle work is biochemically and thermodynamically constrained to cost metabolic energy (Barclay, 2015). The hypothesized cost of force rate therefore needs to be quantified alongside the actual shortening work performed by fascicles.

The present study is intended to address that gap, by testing for a metabolic cost of cyclic force production while accounting for and estimating the costs for mechanical work and force. We

University of Calgary, Faculty of Kinesiology, Biomedical Engineering Graduate Program, Calgary, AB, Canada, T2N 1N4.

*Author for correspondence (tim.vanderzee@ucalgary.ca)

T.J.v.d.Z., 0000-0001-9037-2366; A.D.K., 0000-0001-5233-9709

Received 25 August 2020; Accepted 3 March 2021

Journal of Experimental Biology (2021) 224, jeb233965. doi:10.1242/jeb.233965

simultaneously quantified work (against series elasticity), force and force rate during a cyclic force production task, along with the overall metabolic energy expenditure. The task was to cyclically produce voluntary knee extension torque against an isometric dynamometer, at an amplitude and range of frequencies comparable to everyday human movements. We hypothesized that (1) work and force–time integral fall short in accounting for metabolic cost at higher frequencies, and (2) the surplus cost is related to muscle force rate. We tested this by parametrically relating each contribution as a function of waveform frequency, and testing whether the cost of force rate is separable from and comparable to the costs of work and force–time integral.

MATERIALS AND METHODS

We estimated quadriceps muscle force and mechanical work, and net metabolic rate as healthy adults produced cyclic, isometric knee extension torque (Fig. 1). Increasing frequency of cyclic torque was expected to yield greater fluctuations in muscle force and thereby greater rate of force development. We conducted a set of energetics trials to test for an associated metabolic cost, and a briefer set of mechanics trials to quantify muscle fascicle mechanical work (against series elasticity) and force via ultrasound imaging.

Nine healthy participants (6 male, 3 female, leg length=87.4±4.9 cm, body mass=70.6±13.1 kg, mean±s.d.) produced cyclic bilateral knee extension torque against an isometric dynamometer. The task was intended to require approximately 10% of maximal quadriceps muscle force and to impose contraction frequencies f within ranges encountered in daily life (mean 11 N m and 0.5–2.5 Hz, respectively). Real-time visual feedback was displayed to participants, showing measured and target waveforms (Fig. 1) for each frequency, all at a fixed torque range (0–22 N m) from combined legs. Torques were exerted at 20 deg knee flexion (relative to straight leg) and measured with a dynamometer chair (Biodex, Biodex Medical Systems, NY, USA), which was also used to strap and constrain movement of the trunk and legs. As a reference for maximum torque, participants performed maximum voluntary contractions (MVC) with knee extensor and knee flexor muscles at two knee angles (20 and 70 deg). In line with the knee extension torque–angle relationship (e.g. Kulig et al., 1984), extensor MVCs resulted in less torque at a 20 deg knee angle than at a 70 deg knee angle (97±20 versus 221±70 N m). For each condition, we quantified knee torque in terms of its time average $\bar{T}_{knee}$, peak amplitude and peak rate $\dot{T}_{peak}$ (Fig. 1). Peak torque rate $\dot{T}_{peak}$ was estimated from the change in torque from 50% to 150% of average, divided by the time duration of that change. Prior to data collection, participants provided their written informed consent as approved by the University of Calgary Conjoint Health Research Ethics Board.

The energetics trials entailed cyclic torque production while respirometry data were recorded. Participants were first given practice with matching real-time torque targets for at least 5 min. They then performed the six experimental task conditions for 6 min each, with torque and respirometry (rates of oxygen consumption $\dot{V}_{O_2}$ and carbon dioxide production $\dot{V}_{CO_2}$; K5 system, Cosmed, Rome, Italy) averaged only for the final 3 min, to allow time for oxygen kinetics to stabilize (Xu and Rhodes, 1999). Metabolic rate was determined from $\dot{V}_{O_2}$ and the respiratory exchange ratio (RER, i.e. the ratio between $\dot{V}_{CO_2}$ and $\dot{V}_{O_2}$) (Brockway, 1987). We also recorded electromyography (EMG) to monitor muscle activity and co-contraction [vastus lateralis (VL), rectus femoris (RF) and biceps femoris (BF)]. VL and BF EMG were recorded bilaterally and were averaged between legs, RF EMG was recorded unilaterally. EMG amplitude was determined from the band-pass filtered recordings (cut-off frequency f_c=30–500 Hz, Butterworth) and low-pass filtered to obtain the envelope (f_c=5 Hz, Butterworth) (Hof, 1984). EMG amplitude was defined as the absolute of the Hilbert transformed signal (Huang et al., 1998), expressed relative to its maximum value during MVC and corrected for background noise using baseline subtraction (La Delfa et al., 2014). In addition to waveform targets, there was also a constant torque target of 11 N m to determine the cost of steady force production, with the same average torque as the waveform targets. To avoid potential ordering effects such as from fatigue, the order of task conditions was randomized, with at least 1 min of rest between conditions.

The separate mechanics trials employed ultrasound imaging to estimate muscle fascicle shortening and muscle work against series elasticity. These trials consisted of single-legged isometric torque production with a low-frequency triangle waveform torque target (f=0.02 Hz, range=0–16 N m) at three knee angles (θ_{knee}=15, 20 and 25 deg). The low-frequency mechanics trials were to simplify tracking of images across a range of torques encompassing those

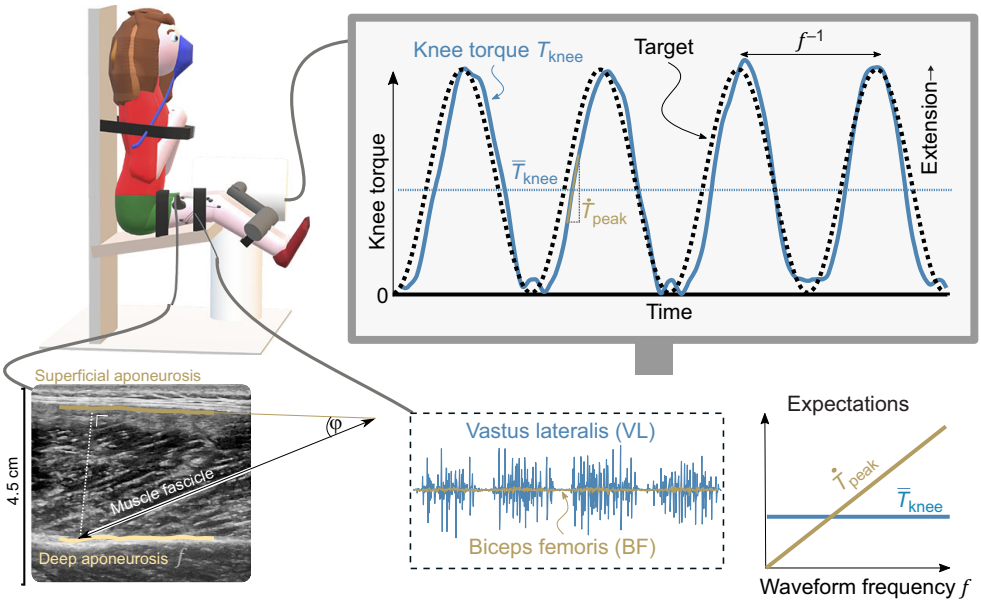

Fig. 1. Experimental set-up for estimating metabolic cost of cyclic, isometric torque production. Participants produced knee extension torque to match a displayed waveform target, while respirometry, electromyography and ultrasound were recorded. Vastus lateralis fascicle length and pennation angle were estimated from ultrasound, and combined with dynamometer to estimate quadriceps muscle force and work (against series elasticity). Sinusoidal torques of increasing waveform frequency f (and fixed amplitude) were expected to result in increasing peak torque rate $\dot{T}_{peak}$ and fixed mean knee torque $\bar{T}_{knee}$, and therefore increasing muscle force rate and energetic cost.

Journal of Experimental Biology (2021) 224, jeb233965. doi:10.1242/jeb.233965

applied in the higher frequency energetics trials. They yielded a force–displacement relationship for fascicle shortening, which could then be used to estimate the shortening work performed during the energetics trials. Images were obtained for the VL using ultrasound (5 cm probe, 11 MHz basic-mode; Logiq E9, General Electric, Fairfield, USA), recorded at 30 Hz and approximately synchronized with torque recordings (via a sync pulse). Separate trials were performed for each of both legs and then averaged between legs. On one occasion, data from one of the legs were discarded owing to poor image quality.

VL fascicle lengths L_{fas} and pennation angles ϕ were estimated using a custom (MathWorks, Natick, MA, USA) ultrasound algorithm (van der Zee and Kuo, 2020 preprint), similar to a previously described algorithm (Ryan et al., 2019). Our algorithm first filtered the images to highlight line-like structures, namely, fascicles and aponeuroses, with thin and thick lines, respectively. The filtered images were then thresholded, and overall fascicle angle was determined using a line detection technique termed Hough transform (Zhou et al., 2015, 2012; Zhou and Zheng, 2008). Aponeuroses were identified using feature detection based on object length, orientation and position. Superficial and deep aponeurosis were identified as the longest object with near-horizontal orientation within the top and bottom image halves, respectively (for details, see van der Zee and Kuo, 2020 preprint). Identified aponeuroses were checked using visual inspection. ϕ was defined as the difference between fascicle angle and superficial aponeurosis angle. L_{fas} was estimated as the distance between deep and superficial aponeuroses, as measured along the fascicle orientation. The junction between fascicle and superficial aponeurosis was linearly extrapolated in the typical case when it was beyond the image frame (see Fig. 1). This procedure was performed for 17 equidistantly spaced locations across the image width to yield an average L_{fas} per image.

At fixed muscle–tendon complex (MTC) length, the change in series elastic element (SEE) length is equal and opposite to the change in the fascicle length along the MTC. Consequently, the SEE length changes ΔL_{SEE} could be estimated from changes in L_{fas} and ϕ (both sampled as a function of T_{knee} at 450 uniformly spaced points) (Fukunaga et al., 2001). At fixed knee torque T_{knee} (and thus fixed F_{SEE}), the change in MTC length is equal and opposite to the change in the fascicle length along the MTC. Consequently, the MTC length changes could be estimated from changes in L_{fas} and ϕ. The moment arm r_{MTC} of the quadriceps MTC about the knee (at θ_{knee}=20 deg) was estimated from the average difference in MTC length between the 15 and the 25 deg trials, divided by the corresponding knee angle difference (i.e. $\Delta\theta_{knee}$=10 deg), similar to typical tendon excursion methods (Ito et al., 2000). Quadriceps MTC force F_{MTC} and its peak rate $\dot{F}_{peak}$ were estimated as knee torque T_{knee} and its peak rate $\dot{T}_{peak}$ divided by moment arm r_{MTC}. SEE force F_{SEE} was assumed to equal quadriceps MTC force F_{MTC}.

The effects of knee torque T_{knee} on muscle fascicle length change ΔL_{fas} and pennation angle change $\Delta\phi$, as well as the effect of SEE force F_{SEE} on SEE length change ΔL_{SEE} were averaged across knee angles and fitted using exponentials. An exponential toe region was used for the SEE force–length curve, appropriate for the relatively low torque levels, less than 10% of maximal torque (Kulig et al., 1984; Lichtwark and Wilson, 2008). The mechanical work done on the SEE by the quadriceps muscle fascicles (W_{fas}) was quantified by the integral of the (fitted) SEE force F_{SEE} with respect to the (fitted) SEE length L_{SEE}, for the torques applied during the energetics trials. Fits were done for each subject individually; work estimates were averaged across subjects.

We hypothesized that overall metabolic cost should include contributions from muscle force rate $\dot{F}$, as well as from mechanical work and steady force production. The force-rate cost was hypothesized to be a consequence of additional active calcium transport by sarco-endoplasmic reticulum calcium ATPase (SERCA) owing to increased myoplasmic calcium concentration (see Fig. 2). Based on imaging and modeling studies (Baylor and Hollingworth, 2012), myoplasmic calcium concentration was expected to increase with force rate (Fig. 2B) owing to rate-limiting dynamics between calcium and muscle force production (Fig. 2A), which act like a low-pass filter. This means that greater amplitudes of calcium should be required to produce a given amount of force at faster rates. (Technically, active transport occurs with muscle deactivation, but only as a consequence of activation, hence our term 'activation cost'.) This general concept is illustrated with an example time constant of 30 ms (Fig. 2B), typical for human force development (Maffiuletti et al., 2016).

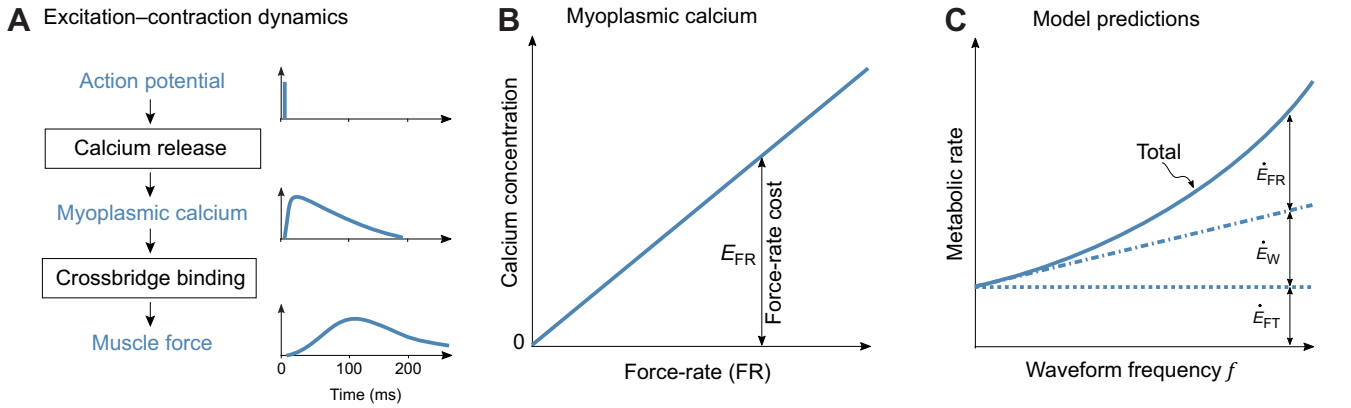

Fig. 2. Hypothesized mechanism for force-rate cost. (A) Excitation–contraction dynamics start with an action potential that triggers calcium release into the myoplasm, which enables crossbridge binding and muscle force production. The rate-limiting effect of crossbridge binding is illustrated by hypothetical transients of action potential, myoplasmic calcium and muscle force versus time. (B) The excitation–contraction dynamics require increasingly large input (myoplasmic calcium) amplitudes, for cyclic force production at faster rates and constant amplitude. As demonstration, this is modeled as a first-order dynamical system (τ=30 ms), with greater calcium (e.g. via recruitment of additional motor units) costing energy for active transport following force production (i.e. 'force-rate cost' E_{FR}). (C) This results in greater metabolic cost per muscle contraction, as well as per time. Associated metabolic rate $\dot{E}_{FR}$ for force rate (FR) is expected to increase quadratically with waveform frequency. In contrast, metabolic rate for force maintenance $\dot{E}_{FT}$ and mechanical work $\dot{E}_{W}$ (FT for force–time integral, W for work) are expected to remain fixed and increase linearly, respectively.

Journal of Experimental Biology (2021) 224, jeb233965. doi:10.1242/jeb.233965

The force-rate cost hypothesis may be expressed as a metabolic cost per contraction, and experimentally tested in terms of a metabolic rate (or cost per time). The cost per muscle contraction E_{FR} should increase in proportion to how quickly the force F increases:

$$E_{FR} \propto \dot{F}, \quad (1)$$

and particularly the peak force rate $\dot{F}_{peak}$. For a sinusoidal force waveform of fixed amplitude, peak force rate is expected to increase with waveform frequency f:

$$\dot{F}_{peak} \propto f. \quad (2)$$

Under steady-state conditions, the corresponding metabolic rate $\dot{E}_{FR}$ (Fig. 2C) depends on the cost per contraction E_{FR} and on the frequency of contractions, yielding:

$$\dot{E}_{FR} \propto E_{FR} \cdot f \propto \dot{F}_{peak} \cdot f \propto f^2. \quad (3)$$

The work and force–time contributions should have separable dependencies on frequency f. Despite an isometric joint, muscle fascicles perform work against series elastic tissues and imperfectly rigid leg and dynamometer. For a fixed torque amplitude, work should be performed in a fixed amount per contraction, and the rate of mechanical work $\dot{W}$ should therefore increase with the rate of contractions, or waveform frequency f. Assuming fixed biochemical costs for fascicle work, the corresponding metabolic rate $\dot{E}_W$ for work production should increase as:

$$\dot{E}_W \propto f^1. \quad (4)$$

The force maintenance contribution is for energy expended even when muscle fascicles are isometric. Metabolic cost should be proportional to the force amplitude and duration of force (or force–time integral; Crow and Kushmerick, 1982). Owing to constant amplitude of the waveform, average knee torque $\bar{T}_{knee}$ and therefore average muscle force were expected to be independent of waveform frequency. The corresponding force–time metabolic rate $\dot{E}_{FT}$ should be independent of waveform frequency:

$$\dot{E}_{FT} \propto f^0. \quad (5)$$

In our experiments, we tested for an overall metabolic cost with all three of these contributions. We hypothesized that net metabolic rate $\dot{E}_{net}$ would be the sum of force rate, work and force–time integral terms:

$$\dot{E}_{net} = \dot{E}_{FR} + \dot{E}_W + \dot{E}_{FT} = c_2 f^2 + c_1 f^1 + c_0 f^0, \quad (6)$$

where 'net' is defined as gross minus the cost of quiet sitting. We assumed differences in net metabolic rate $\dot{E}_{net}$ to mainly reflect knee muscle energy consumption, as producing low forces should have negligible effects on metabolism in other muscles (e.g. cardiovascular) and organs. The expected cost of performing fascicle work is derived from the inverse product of the efficiencies of (1) obtaining ATP from food stuff (about 60%; van Ingen Schenau et al., 1997) and (2) crossbridge formation (about 50%; Barclay, 2015), yielding the linear coefficient c_1 of 3.33. The other coefficients (c_0 and c_2) were determined using regression with f as the independent variable. Unless stated otherwise, standard deviations (s.d.) refer to between-subjects variability.

RESULTS

Prior to examining the metabolic rate of cyclic force production, we first examined the experimental conditions, which showed that participants matched target torques well. As expected, participants' knee torque $T_{knee}(t)$ resembled a sinusoidal waveform, with constant average $\bar{T}_{knee}$ and variable peak rate $\dot{T}_{peak}$. There was no significant dependency of waveform frequency f on average torque $\bar{T}_{knee}$ (slope 0.2±0.4 N m Hz^{-1}, mean±95% CI, P=0.5, linear regression). Average knee torque $\bar{T}_{knee}$, torque minima and maxima were 10.7±1.0, 1.0±1.0 and 21.8±1.2 N m, respectively (means±s.d. across subjects and conditions; Fig. 3A). Average knee torque $\bar{T}_{knee}$ was 11.6±0.7 N m (mean±s.d.) in the constant torque condition. Despite constant average torque $\bar{T}_{knee}$, quadriceps EMG amplitude increased with waveform frequency by about 76% (VL: 2.1±0.5% MVC at 0.5 Hz to 3.7±0.6% MVC at 2.5 Hz, mean±s.d.). The increase was approximately linear in frequency f, at rates of 0.8±0.3, 1.0±0.3 and 0.2±0.1% MVC Hz^{-1} for VL, RF and BF, respectively (means±95% CI, repeated-measures linear regression). Averaged across conditions, VL EMG amplitude was

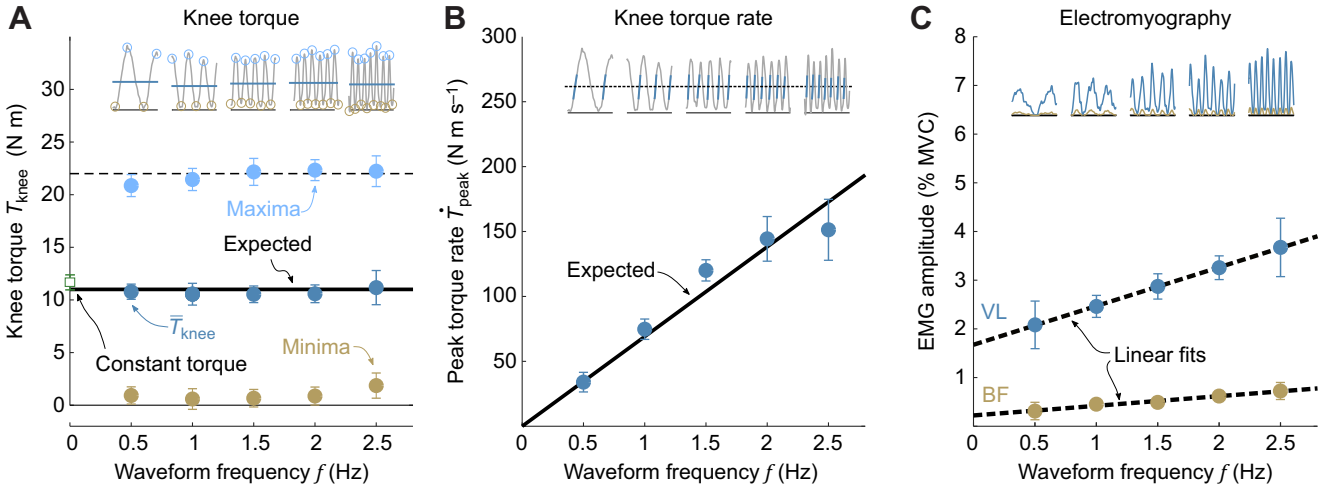

Fig. 3. Experimentally measured torque, torque rate and electromyography (EMG) versus waveform frequency. (A) Knee torque versus waveform frequency f, in terms of time average, minima and maxima of waveforms (shown in insets). Time-averaged torque $\bar{T}_{knee}$ was relatively constant across conditions, comparable to the expected 11 N m. (B) Peak torque rate versus waveform frequency f. Torque rate $\dot{T}_{peak}$ (shown in inset) increased with frequency f, comparable to expected (solid line). (C) EMG amplitudes versus frequency f, for vastus lateralis (VL) and biceps femoris (BF) averaged between legs. EMG amplitude increased approximately linearly with waveform frequency. Filled symbols denote means across subjects (N=9); error bars denote ±s.d.

1.0±2.4% MVC higher in the left leg than in the right leg. There was no difference in BF EMG amplitude between legs (i.e. 0.0±0.3% MVC difference). There was some co-contraction, with BF EMG amplitude less than 1% MVC in all conditions (Fig. 3C), on average approximately one-eighth of VL EMG amplitudes. Peak knee torque rate $\dot{T}_{peak}$ increased with waveform frequency f (slope 68.3±3.4 N m, mean±95% CI, linear regression without offset), and closely resembled the increase expected from the torque targets (slope 69.1 N m, R^2=0.84, Fig. 3B).

Quadriceps muscle fascicles performed work during isometric torque production, as evidenced by VL fascicle shortening (Fig. 4A) and pennation angle changes (Fig. 4B) observed during mechanics trials. All results reported here are averaged between legs, unless stated otherwise. As a baseline, VL fascicle length was estimated at 9.5±0.8 cm (mean±s.d.) during rest (20 deg knee flexion). Fascicle lengths decreased with greater torque, as described by a fitted exponential (R^2=0.36; see Fig. 4A). At 11 N m, muscle fascicles had shortened by 1.4±0.6 cm. Pennation angle increased with greater torque, also described by a fitted exponential (R^2=0.36; Fig. 4B). Pennation angle was 15.9±1.2 deg (mean±s.d.) at rest, and increased by 3.4±1.1 deg at 11 N m. Combining fascicle length and pennation angle changes with knee angle, quadriceps MTC moment arm r_{MTC} was estimated at 5.0±1.9 cm (mean±s.d.). These data also yielded an estimate of length change of SEEs, fitted by an exponential toe region (R^2=0.37; Fig. 4C). From that fit, quadriceps muscle fascicle work W_{fas} was estimated at 1.2±0.6 J (mean±s.d.) for an 11 N m contraction. The same estimate was obtained when exclusively using left leg data (1.2±0.8 J) or right leg data (1.2±0.7 J). Using the measured cyclic torque maxima (see Fig. 3A) instead of assuming 11 N m contractions resulted in similar work estimates (see Fig. 5A). The increase in mechanical work rate $\dot{W}_{fas}$ with waveform frequency was therefore approximately 2.4±1.2 J.

Net metabolic rate $\dot{E}_{net}$ increased with waveform frequency f (P=4×10^{-6}, repeated-measures regression; Fig. 5B), in agreement with predictions. The RER was below 0.8 in all conditions, indicating aerobic metabolism. Net metabolic rate $\dot{E}_{net}$ increased from a value of 10.5±13.2 W (mean±s.d.) at the lowest frequency (f=0.5 Hz) to 46.8±8.3 W at the highest frequency (f=2.5 Hz). The overall cost appeared to agree with hypothesized contributions from force rate $\dot{E}_{FR}$, work $\dot{E}_{W}$ and force–time $\dot{E}_{FT}$. At the highest frequency, these three costs were estimated at 18.9, 20.1 and 7.8 W, respectively, or approximately 40.4%, 43.0% and 16.6% of net metabolic rate $\dot{E}_{net}$. Costs of force rate $\dot{E}_{FR}$ and force–time $\dot{E}_{FT}$ had coefficients of 3.2±0.6 J s and 7.8±2.2 W, respectively (mean±95% CI, P=9×10^{-6} and P=0.001, respectively, linear mixed-effects regression). The force–time cost estimate $\dot{E}_{FT}$ was comparable to the metabolic cost of the constant torque condition (9.8±12.7 W, mean±s.d.). Examining the force-rate cost as a cost per contraction E_{FR} (Fig. 5C), it increased linearly with measured peak force rate $\dot{F}_{peak}$ (2.6±1.9×10^{-3} m s, mean±95% CI, linear mixed-effects regression without offset, P=0.008; Fig. 5C).

DISCUSSION

The present study aimed at investigating the metabolic cost related to muscle force rate, separately from both force and mechanical work costs. Net metabolic rate increased with the frequency of isometric torque production, faster than would be expected for force production alone. We also estimated muscle fascicle shortening, and observed non-negligible work performed by fascicles, but also insufficient to explain metabolic cost. A considerable portion of the overall metabolic cost can be ascribed to the proposed force-rate cost. We next examined the hypothesis in relation to the data, the potential mechanisms for the force-rate cost, and implications for movement.

We first considered why force and work production alone do not explain the observed metabolic cost. The cyclic, isometric task resulted in nearly the same average force across conditions. The muscle force–time integral was therefore unchanged across frequencies, and likely to have the same metabolic cost in all conditions. The force–time cost estimate accounted for 74% of metabolic cost in the 0.5 Hz condition, as opposed to only 17% in the 2.5 Hz condition. Expressed as a cost per unit force, the force–time cost estimate (i.e. 0.038 W N^{-1}) is well within the range of values reported previously (i.e. 0.020–0.058 W N^{-1}, Ortega et al., 2015; van der Zee et al., 2019). Muscle co-contraction could

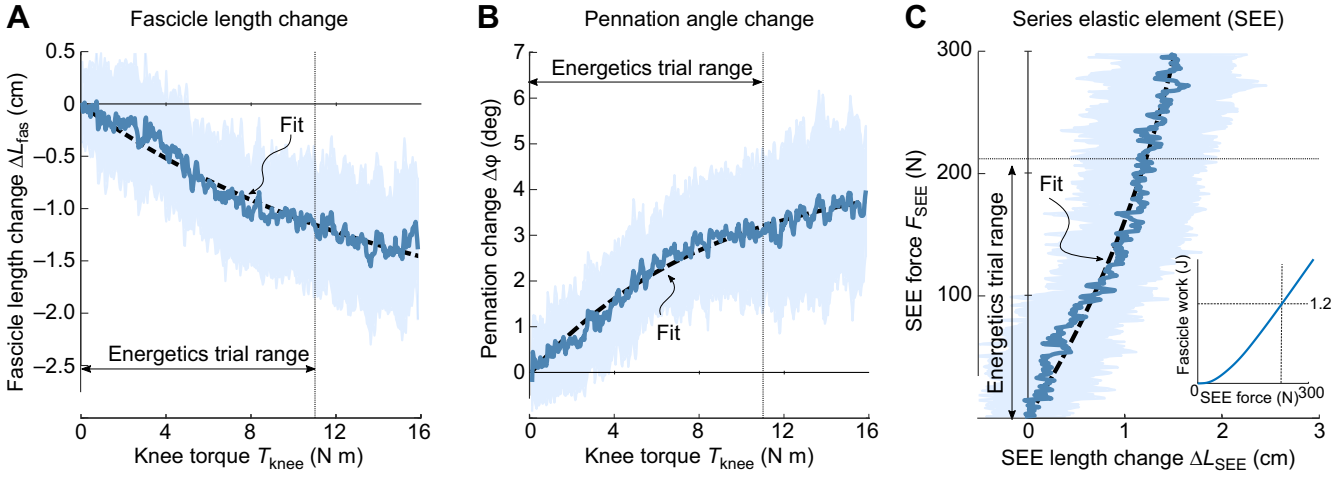

Fig. 4. Muscle fascicle and series elastic element (SEE) elongation as a function of knee torque. (A) Muscle fascicle length change (relative to relaxed) ΔL_{fas} versus knee torque T_{knee}. Fascicle length decreased with greater knee torque, with exponential fit. (B) Muscle pennation angle change $\Delta\phi$ versus knee torque torque T_{knee}. Pennation angle increased with greater knee torque, with exponential fit. (C) SEE force F_{SEE} versus length change ΔL_{SEE}. SEE length increased with greater SEE force, with fit to exponential toe region. Inset: resulting fit was used to estimate mechanical work done by fascicles during the energetics trials. Data here were obtained during isometric mechanics trials, based on fascicle shortening. All results shown here are averaged between legs. Dark lines indicate means across subjects (N=9); shaded area denotes ±s.d.

Journal of Experimental Biology (2021) 224, jeb233965. doi:10.1242/jeb.233965

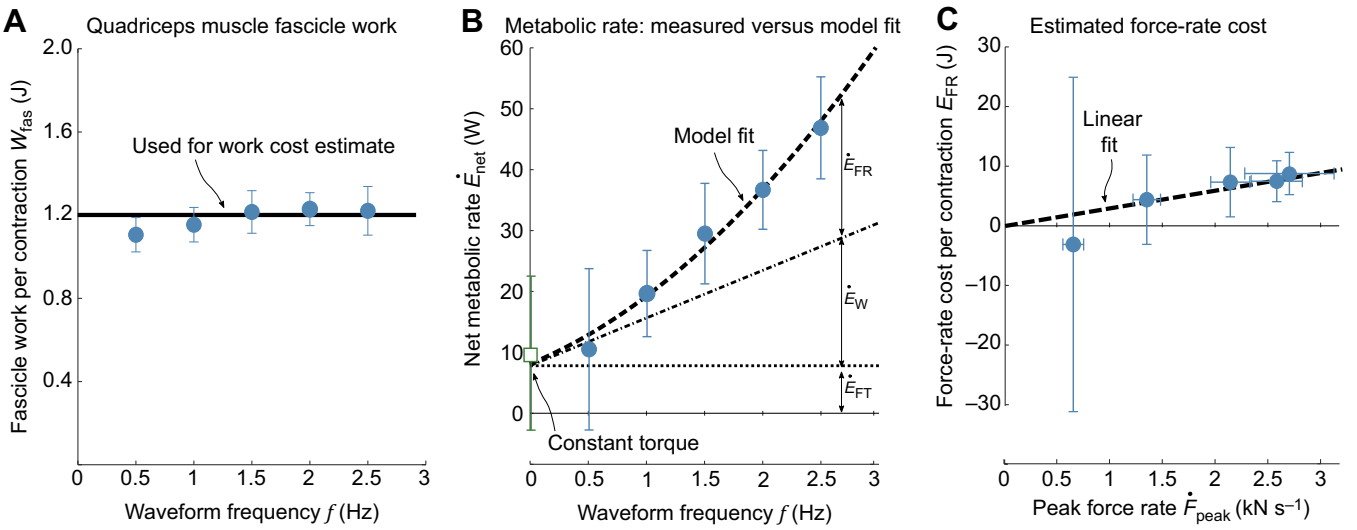

Fig. 5. Metabolic cost of cyclic force production. (A) Quadriceps muscle fascicle work versus waveform frequency *f*. Work estimate derived from series elastic element force–length curve (Fig. 4C), either assuming a 11 N m contraction (solid line) or using the measured torque maxima (data points). (B) Net metabolic rate $\dot{E}_{net}$ versus waveform frequency *f*, along with three separate hypothesized contributing terms: (1) a force–time term $\dot{E}_{FT}$ independent of *f*, (2) a work term $\dot{E}_{W}$ increasing linearly with *f*, and (3) the hypothesized force-rate term $\dot{E}_{FR}$, increasing with f^2. Net metabolic rate $\dot{E}_{net}$ increased with waveform frequency (P=4×10^{-6}) and was largely explained by a quadratic fit (R^2=0.66) with the linear coefficient fixed to the cost of work coefficient c_1. (C) Force-rate cost per contraction E_{FR} versus measured peak force rate $\dot{F}_{peak}$. As hypothesized (see Fig. 2), E_{FR} (isolated from force–time and work terms) increased linearly with measured $\dot{F}_{peak}$ (P=0.008). Filled symbols denote means across subjects (N=9); error bars denote ±s.d.

have affected the force–time cost, as antagonist force needs to be offset by additional agonist force. We did observe antagonist EMG of relatively small and linearly increasing amplitude, but consider it unlikely to explain the quadratically increasing energetic cost with waveform frequency. The cost of steady isometric contraction has in part been ascribed to muscle crossbridges, which cycle even when net work is zero (Barclay et al., 2007), with energy dissipated as heat. The force–time coefficient c_0 in part reflects such dissipative crossbridge cycling in isometric conditions. As shortening velocity increases, a smaller fraction of metabolic energy is dissipated as heat, while a greater fraction is converted into mechanical work (Barclay et al., 2010). This suggests that we may have overestimated the force–time coefficient c_0 at higher waveform frequencies. Although the force–time cost did not increase with waveform frequency, the mechanical work rate did increase. We assumed a proportional work cost, implying a constant crossbridge efficiency. However, crossbridge efficiency is thought to increase with shortening velocity, peaking at approximately 15–25% of maximal shortening velocity (Smith et al., 2005). This increase is thought to reflect more work done per crossbridge cycle owing to an increased working stroke length with crossbridge strain similar to isometric values (Barclay et al., 2010), implying fewer active crossbridges per unit work. Assuming previously reported muscle optimal length and maximal shortening velocity (De Ruiter et al., 2000; van Soest et al., 1993), shortening velocities in the present study were always well below 15% of maximal shortening velocity. Consequently, if anything, crossbridge efficiency would have increased with waveform frequency. Therefore, we may have overestimated the work cost at higher waveform frequencies by assuming a fixed mechanical efficiency. Altogether, the assumptions we have applied would lead to overestimation of work and/or force–time costs, so that their sum might actually explain less than the 60% of net metabolic cost we have estimated.

This leaves a substantial cost explained by the hypothesized force-rate cost. The sharp increase in metabolic cost with muscle contraction frequency (Fig. 5) was consistent with the expected force-rate cost increasing with the square of contraction frequency. The hypothesis is based on the rate-limited dynamics between muscle excitation and force production, which acts as a low-pass filter of excitation and associated calcium release into the myoplasm. In the present experiment, increasing contraction frequencies called for higher force rates ($\dot{F}$, Fig. 3), which are expected to require more calcium release per muscle contraction. Active calcium pumping returns the calcium to the sarcoplasmic reticulum, with an associated metabolic cost (SERCA; Inoue et al., 2019). This contrasts with the energetic costs for force maintenance or work production, both associated with cycling of actomyosin crossbridges (actomyosin ATPase). Our hypothesis is that the combination of rate-limiting dynamics and calcium pumping imply a separate force-rate cost. This cost is in addition to the traditional force- and work-related costs, and could explain 40% (or more, if work and force–time costs are overestimated) of metabolic cost observed at the higher frequencies of the present experiment. In movement conditions that require cyclic muscle contraction, the force-rate cost could be quite substantial.

A potential source of uncertainty is imaging of VL fascicle length and pennation angle. Fascicle angle estimates obtained from the Hough transform have been found to correlate well with traditional (manual) estimates (Zhou et al., 2015, 2012; Zhou and Zheng, 2008). Different in the current algorithm was the (semi-)automated muscle thickness estimation from aponeurosis objects identified using feature detection. To avoid erroneous muscle thickness estimates, identified aponeurosis objects were visually inspected and corrected where necessary. Owing to the VL fascicles extending beyond the ultrasound image frame, we linearly extrapolated fascicles to an aponeurosis point outside the frame (Brennan et al., 2017). To avoid excess linear extrapolation, we selected conditions (20 deg knee angle) to keep fascicles at relatively short length (Marzilger et al., 2018). To ensure clear images, we used a slow waveform frequency for torque production. Our quadriceps muscle work estimate was the same when exclusively using left leg versus right leg data, suggesting good consistency across legs. The

resulting estimates of fascicle shortening (approximately 1.4 cm) were comparable to manually obtained estimates under comparable conditions (Fukunaga et al., 1997; Ichinose et al., 1997).

We used knee torque, VL fascicle length and VL pennation angle to estimate quadriceps muscle work against SEEs during isometric torque production. We assumed that SEE length changes, as estimated from VL fascicle shortening, were shared across the quadriceps heads, which all have a common distal tendon. Each head also has its own aponeurosis, which we assumed would not drastically affect our results. Similar activation patterns have been observed between VL and vastus medialis by others (Wakeling and Horn, 2009). While activation can differ between rectus femoris and vastii in some conditions (Wakeling and Horn, 2009), we observed quite comparable EMGs for VL and rectus femoris for the conditions in the present study. We also assumed equal contributions of left and right leg to knee torque. While left and right leg EMG increased to similar extents with waveform frequency, their average values were different. However, even if there was a difference in contribution between legs, this would not have affected the work estimate because the work–force curve was approximately linear around the peak forces during the cyclic force experiment (see Fig. 4C, inset). Our ultrasound estimates can also be compared against two alternatives. One is to assume that muscle fascicles do not shorten against an isometric dynamometer, thus yielding zero work. Another is to consult the literature for SEE stress–strain curves. Assuming 4–5% SEE strain at maximal muscle force (e.g. Millard et al., 2013), a SEE slack length of 20 cm (based on VL and RF values in van Soest and Bobbert, 1993) and a typical toe region (Thelen, 2003), a contraction at 10% of maximal muscle force would perform 0.24 J of work against SEE, 5 times less than we reported. This discrepancy may in part reflect an overestimation of work in the present study. Altogether, potential inaccuracies in our quadriceps muscle work estimate would lead to an overestimate of work and its energetic cost. This would suggest that the hypothesized force-rate cost is greater than estimated here.

Evidence for the proposed force-rate cost has previously been demonstrated in both muscle and whole-body experiments. For cyclic isometric contraction of mouse muscle *in situ* (1:3 on:off duty factor), rate of oxygen consumption is higher when cycle frequency is higher (Hogan et al., 1998). For prolonged isometric contraction of human VL muscle *in vivo*, rate of ATP utilization is higher when stimulation is cyclic (1:1 on:off duty factor) compared with constant (Chasiotis et al., 1987; Spriet et al., 1988). For cyclic isometric contraction of human calf muscle at constant frequency, metabolic cost decreases with increasing duty factor (Beck et al., 2020). While these studies have indicated a metabolic cost for cyclic muscle contraction, this cost was not parametrically related to muscle force-rate. We believe that force rate, rather than work or force–time, could explain many such findings on metabolic cost of cyclic isometric contraction. In contrast to previous studies on isometric contraction varying on–off durations, we parametrically related such metabolic cost to muscle force rate, which we find more suitable for the continuously varying forces of most daily movements. Furthermore, metabolic cost of cyclic movement has been observed to increase with movement frequency in leg swinging (Doke et al., 2005; Doke and Kuo, 2007), ankle bouncing (Dean and Kuo, 2011) and arm reaching (Wong et al., 2020 preprint). Altogether, the force-rate cost seems to be observable during a variety of movements and contraction conditions. Here, we provide evidence that the force-rate cost exists during voluntary isometric contraction, independently of work and force–time costs.

We have separated total metabolic cost into three terms: work, force time and force rate. Such phenomenological division is potentially explained mechanistically as costs due to individual ATPases, particularly actomyosin (for work and force time) and SERCA (for force rate). Whether SERCA is primarily responsible for the force-rate cost could be tested in future experimental studies on isolated muscle, for example using crossbridge (and therefore actomyosin ATPase) blocking agents (Barclay et al., 2007). We expect SERCA ATP consumption rate to increase with contraction frequency because of the increase in calcium release amplitudes, owing to rate-limiting force production dynamics. Higher calcium amplitudes would require higher muscle activation levels, which agrees with the observed increase in quadriceps EMG amplitude with waveform frequency. Such properties are not included in Hill-type muscle models (Zajac, 1989), which do have activation dynamics attributed to calcium release (sometimes called 'active state') and muscle force–length and –velocity dependency, but not rate-limiting dynamics between calcium release and muscle force. As demonstration, we simulated the present experiment with a commonly used metabolic muscle model (OpenSim software, Uchida et al., 2016). It predicted a 2.4 W increase in metabolic rate with waveform frequency, only approximately 7% of the amount experimentally measured. Current models therefore appear to underestimate the energetic cost of cyclic force production. Improved estimates might be obtained by including rate-limiting dynamics, crudely modeled as a low-pass filter here, such as calcium release and binding (Baylor and Hollingworth, 2012) and Huxley-type crossbridge binding (van Soest et al., 2019). Future modeling studies could develop such mechanistic models that explain the force-rate cost.

Fast contraction of muscle may require high calcium release and pumping rates, at the cost of metabolic energy spend by SERCA. Such energetic penalty for rapid increase in muscle force may explain why (ground reaction) forces during human walking are smoother than expected based on work considerations (Rebula and Kuo, 2015). Nevertheless, there may be a considerable force-rate cost during human locomotion, as VL fascicles produce relatively short bursts of high force without shortening much (0–30% of stride; Bohm et al., 2018). The force-rate cost may also apply to a variety of other animals. In locust flight muscle, oxygen consumption during cyclic isometric contraction is 87% of the consumption during maximal power output, indicating a high cost for cyclic muscle activation (Josephson and Stevenson, 1991). Locusts use synchronous muscle with one contraction per wing beat, whereas other insects such as beetles use asynchronous muscle with fewer contractions per beat (Josephson et al., 2001), which could reduce the activation cost as a potentially advantageous adaptation (Syme and Josephson, 2002). A force-rate cost could be an important factor in energy expenditure in a wide range of movements and species.

Conclusions

We observed an increase in average net metabolic rate with frequency of cyclic torque production, which could not be explained by force–time nor by muscle fascicle mechanical work. Average net metabolic rate was related to force rate, suggesting that increasing muscle force abruptly requires more metabolic energy than when done slowly. We propose that this metabolic cost of force rate may be explained by an increase in the amount of required active calcium transport, and may be relevant for a wide range of movements.

Acknowledgements

The authors would like to thank Ashna Subramanium for assistance with data collection.

Competing interests

The authors declare no competing or financial interests.

Author contributions

Conceptualization: T.J.v.d.Z., A.D.K.; Methodology: T.J.v.d.Z., A.D.K.; Software: T.J.v.d.Z.; Validation: T.J.v.d.Z., A.D.K.; Formal analysis: T.J.v.d.Z.; Investigation: T.J.v.d.Z.; Resources: A.D.K.; Data curation: T.J.v.d.Z.; Writing - original draft: T.J.v.d.Z.; Writing - review & editing: T.J.v.d.Z., A.D.K.; Visualization: T.J.v.d.Z., A.D.K.; Supervision: A.D.K.; Project administration: A.D.K.; Funding acquisition: A.D.K.

Funding

This work was supported in part by the Natural Sciences and Engineering Research Council of Canada (NSERC Discovery and Canada Research Chair, Tier 1) and the Dr Benno Nigg Research Chair in Biomechanics.

Data availability

Ultrasound algorithm and typical example of ultrasound data are available from github at: https://github.com/timvanderzee/ultrasound-automated-algorithm

References

Abbott, B. C., Bigland, B. and Ritchie, J. M. (1952). The physiological cost of negative work. *J. Physiol.* **117**, 380-390. doi:10.1113/jphysiol.1952.sp004755

Barclay, C. J. (2015). Energetics of contraction. *Compr. Physiol.* **5**, 961-995. doi:10.1002/cphy.c140038

Barclay, C. J., Woledge, R. C. and Curtin, N. A. (2007). Energy turnover for Ca^{2+} cycling in skeletal muscle. *J. Muscle Res. Cell Motil.* **28**, 259-274. doi:10.1007/s10974-007-9116-7

Barclay, C. J., Woledge, R. C. and Curtin, N. A. (2010). Inferring crossbridge properties from skeletal muscle energetics. *Prog. Biophys. Mol. Biol.* **102**, 53-71. doi:10.1016/j.pbiomolbio.2009.10.003

Baylor, S. M. and Hollingworth, S. (2012). Intracellular calcium movements during excitation–contraction coupling in mammalian slow-twitch and fast-twitch muscle fibers. *J. Gen. Physiol.* **139**, 261-272. doi:10.1085/jgp.201210773

Beck, O. N., Gosyne, J., Franz, J. R. and Sawicki, G. S. (2020). Cyclically producing the same average muscle-tendon force with a smaller duty increases metabolic rate. *Proc. R. Soc. B* **287**, 20200431. doi:10.1098/rspb.2020.0431

Bergström, M. and Hultman, E. (1988). Energy cost and fatigue during intermittent electrical stimulation of human skeletal muscle. *J. Appl. Physiol.* **65**, 1500-1505. doi:10.1152/jappl.1988.65.4.1500

Bohm, S., Marzilger, R., Mersmann, F., Santuz, A. and Arampatzis, A. (2018). Operating length and velocity of human vastus lateralis muscle during walking and running. *Sci. Rep.* **8**, 5066. doi:10.1038/s41598-018-23376-5

Brennan, S. F., Cresswell, A. G., Farris, D. J. and Lichtwark, G. A. (2017). *In vivo* fascicle length measurements via B-mode ultrasound imaging with single vs dual transducer arrangements. *J. Biomech.* **64**, 240-244. doi:10.1016/j.jbiomech.2017.09.019

Brockway, J. M. (1987). Derivation of formulae used to calculate energy expenditure in man. *Hum. Nutr. Clin. Nutr.* **41**, 463-471.

Chasiotis, D., Bergström, M. and Hultman, E. (1987). ATP utilization and force during intermittent and continuous muscle contractions. *J. Appl. Physiol.* **63**, 167-174. doi:10.1152/jappl.1987.63.1.167

Crow, M. T. and Kushmerick, M. J. (1982). Chemical energetics of slow- and fast-twitch muscles of the mouse. *J. Gen. Physiol.* **79**, 147-166. doi:10.1085/jgp.79.1.147

De Ruiter, C. J., Didden, W. J. M., Jones, D. A. and De Haan, A. (2000). The force–velocity relationship of human adductor pollicis muscle during stretch and the effects of fatigue. *J. Physiol.* **526**, 671-681. doi:10.1111/j.1469-7793.2000.00671.x

Dean, J. C. and Kuo, A. D. (2011). Energetic costs of producing muscle work and force in a cyclical human bouncing task. *J. Appl. Physiol.* **110**, 873-880. doi:10.1152/japplphysiol.00505.2010

Doke, J. and Kuo, A. D. (2007). Energetic cost of producing cyclic muscle force, rather than work, to swing the human leg. *J. Exp. Biol.* **210**, 2390-2398. doi:10.1242/jeb.02782

Doke, J., Donelan, J. M. and Kuo, A. D. (2005). Mechanics and energetics of swinging the human leg. *J. Exp. Biol.* **208**, 439-445. doi:10.1242/jeb.01408

Fukunaga, T., Ichinose, Y., Ito, M., Kawakami, Y. and Fukashiro, S. (1997). Determination of fascicle length and pennation in a contracting human muscle *in vivo*. *J. Appl. Physiol.* **82**, 354-358. doi:10.1152/jappl.1997.82.1.354

Fukunaga, T., Kubo, K., Kawakami, Y., Fukashiro, S., Kanehisa, H. and Maganaris, C. N. (2001). *In vivo* behaviour of human muscle tendon during walking. *Proc. R. Soc. B Biol. Sci.* **268**, 229-233. doi:10.1098/rspb.2000.1361

Hof, A. L. (1984). EMG and muscle force: an introduction. *Hum. Mov. Sci.* **3**, 119-153. doi:10.1016/0167-9457(84)90008-3

Hogan, M. C., Ingham, E. and Kurdak, S. S. (1998). Contraction duration affects metabolic energy cost and fatigue in skeletal muscle. *Am. J. Physiol.* **274**, E397-E402. doi:10.1152/ajpendo.1998.274.3.E397

Huang, N. E., Shen, Z., Long, S. R., Wu, M. C., Shih, H. H., Zheng, Q., Yen, N.-C., Tung, C. C. and Liu, H. H. (1998). The empirical mode decomposition and the Hilbert spectrum for nonlinear and non-stationary time series analysis. *Proc. Math. Phys. Eng. Sci.* **454**, 903-995. doi:10.1098/rspa.1998.0193

Huang, H. J., Kram, R. and Ahmed, A. A. (2012). Reduction of metabolic cost during motor learning of arm reaching dynamics. *J. Neurosci.* **32**, 2182-2190. doi:10.1523/JNEUROSCI.4003-11.2012

Ichinose, Y., Kawakami, Y., Ito, M. and Fukunaga, T. (1997). Estimation of active force–length characteristics of human vastus lateralis muscle. *Cells Tissues Organs* **159**, 78-83. doi:10.1159/000147969

Inoue, M., Sakuta, N., Watanabe, S., Zhang, Y., Yoshikaie, K., Tanaka, Y., Ushioda, R., Kato, Y., Takagi, J., Tsukazaki, T. et al. (2019). Structural basis of Sarco/Endoplasmic Reticulum Ca^{2+}-ATPase 2b regulation via transmembrane helix interplay. *Cell Rep.* **27**, 1221-1230.e3. doi:10.1016/j.celrep.2019.03.106

Ito, M., Akima, H. and Fukunaga, T. (2000). In vivo moment arm determination using B-mode ultrasonography. *J. Biomech.* **33**, 215-218. doi:10.1016/S0021-9290(99)00154-2

Josephson, R. K. and Stevenson, R. D. (1991). The efficiency of a flight muscle from the locust *Schistocerca americana*. *J. Physiol.* **442**, 413-429. doi:10.1113/jphysiol.1991.sp018800

Josephson, R. K., Malamud, J. G. and Stokes, D. R. (2001). The efficiency of an asynchronous flight muscle from a beetle. *J. Exp. Biol.* **204**, 4125-4139.

Kulig, K., Andrews, J. G. and Hay, J. G. (1984). Human strength curves. *Exerc. Sport Sci. Rev.* **12**, 417-466. doi:10.1249/00003677-198401000-00014

La Delfa, N. J., Sutherland, C. A. and Potvin, J. R. (2014). EMG processing to interpret a neural tension-limiting mechanism with fatigue. *Muscle Nerve* **50**, 384-392. doi:10.1002/mus.24158

Lichtwark, G. A. and Wilson, A. M. (2008). Optimal muscle fascicle length and tendon stiffness for maximising gastrocnemius efficiency during human walking and running. *J. Theor. Biol.* **252**, 662-673. doi:10.1016/j.jtbi.2008.01.018

Maffiuletti, N. A., Aagaard, P., Blazevich, A. J., Folland, J., Tillin, N. and Duchateau, J. (2016). Rate of force development: physiological and methodological considerations. *Eur. J. Appl. Physiol.* **116**, 1091-1116. doi:10.1007/s00421-016-3346-6

Margaria, R. (1968). Positive and negative work performances and their efficiencies in human locomotion. *Int. Z. Angew. Physiol. Einschl. Arbeitsphysiol.* **25**, 339-351. doi:10.1007/BF00699624

Margaria, R. (1976). *Biomechanics and Energetics of Muscular Exercise*. Oxford: Clarendon Press.

Marzilger, R., Legerlotz, K., Panteli, C., Bohm, S. and Arampatzis, A. (2018). Reliability of a semi-automated algorithm for the vastus lateralis muscle architecture measurement based on ultrasound images. *Eur. J. Appl. Physiol.* **118**, 291-301. doi:10.1007/s00421-017-3769-8

Millard, M., Uchida, T., Seth, A. and Delp, S. L. (2013). Flexing computational muscle: modeling and simulation of musculotendon dynamics. *J. Biomech. Eng.* **135**, 021005. doi:10.1115/1.4023390

Ortega, J. O., Lindstedt, S. L., Nelson, F. E., Jubrias, S. A., Kushmerick, M. J. and Conley, K. E. (2015). Muscle force, work and cost: a novel technique to revisit the Fenn effect. *J. Exp. Biol.* **218**, 2075-2082. doi:10.1242/jeb.114512

Rebula, J. R. and Kuo, A. D. (2015). The cost of leg forces in bipedal locomotion: a simple optimization study. *PLoS ONE* **10**, e0117384. doi:10.1371/journal.pone.0117384

Ryan, D. S., Stutzig, N., Siebert, T. and Wakeling, J. M. (2019). Passive and dynamic muscle architecture during transverse loading for gastrocnemius medialis in man. *J. Biomech.* **86**, 160-166. doi:10.1016/j.jbiomech.2019.01.054

Smith, N. P., Barclay, C. J. and Loiselle, D. S. (2005). The efficiency of muscle contraction. *Prog. Biophys. Mol. Biol.* **88**, 1-58. doi:10.1016/j.pbiomolbio.2003.11.014

Spriet, L. L., Soderlund, K. and Hultman, E. (1988). Energy cost and metabolic regulation during intermittent and continuous tetanic contractions in human skeletal muscle. *Can. J. Physiol. Pharmacol.* **66**, 134-139. doi:10.1139/y88-024

Syme, D. A. and Josephson, R. K. (2002). How to build fast muscles: synchronous and asynchronous designs. *Integr. Comp. Biol.* **42**, 762-770. doi:10.1093/icb/42.4.762

Thelen, D. G. (2003). Adjustment of muscle mechanics model parameters to simulate dynamic contractions in older adults. *J. Biomech. Eng.* **125**, 70-77. doi:10.1115/1.1531112

Uchida, T. K., Hicks, J. L., Dembia, C. L. and Delp, S. L. (2016). Stretching your energetic budget: how tendon compliance affects the metabolic cost of running. *PLoS ONE* **11**, e0150378. doi:10.1371/journal.pone.0150378

van der Zee, T. J. and Kuo, A. D. (2020). Fully automated algorithm estimates muscle fascicle length from ultrasound image. *BioRxiv*, 2020.08.23.263574.

van der Zee, T. J., Lemaire, K. K. and van Soest, A. J. (2019). The metabolic cost of *in vivo* constant muscle force production at zero net mechanical work. *J. Exp. Biol.* **222**, jeb199158. doi:10.1242/jeb.199158

van Ingen Schenau, G. J., Bobbert, M. F. and de Haan, A. (1997). Does elastic energy enhance work and efficiency in the stretch–shortening cycle? *J. Appl. Biomech.* **13**, 389-415. doi:10.1123/jab.13.4.389

van Soest, A. J. and Bobbert, M. F. (1993). The contribution of muscle properties in the control of explosive movements. *Biol. Cybern.* **69**, 195-204. doi:10.1007/BF00198959

van Soest, A. J., Schwab, A. L., Bobbert, M. F. and van Ingen Schenau, G. J. (1993). The influence of the biarticularity of the gastrocnemius muscle on vertical-jumping achievement. *J. Biomech.* **26**, 1-8. doi:10.1016/0021-9290(93)90608-H

van Soest, A. J. K., Casius, L. J. R. and Lemaire, K. K. (2019). Huxley-type cross-bridge models in largeish-scale musculoskeletal models; an evaluation of computational cost. *J. Biomech.* **83**, 43-48. doi:10.1016/j.jbiomech.2018.11.021

Wakeling, J. M. and Horn, T. (2009). Neuromechanics of muscle synergies during cycling. *J. Neurophysiol.* **101**, 843-854. doi:10.1152/jn.90679.2008

Wong, J. D., Cluff, T. and Kuo, A. D. (2020). The energetic basis for smooth human arm movements. *BioRxiv*. doi:10.1101/2020.12.28.424067

Xu, F. and Rhodes, E. C. (1999). Oxygen uptake kinetics during exercise. *Sports Med.* **27**, 313-327. doi:10.2165/00007256-199927050-00003

Zajac, F. E. (1989). Muscle and tendon: properties, models, scaling, and application to biomechanics and motor control. *Crit. Rev. Biomed. Eng.* **17**, 359-411.

Zhou, Y. and Zheng, Y.-P. (2008). Estimation of muscle fiber orientation in ultrasound images using revoting Hough transform (RVHT). *Ultrasound Med. Biol.* **34**, 1474-1481. doi:10.1016/j.ultrasmedbio.2008.02.009

Zhou, Y., Li, J.-Z., Zhou, G. and Zheng, Y.-P. (2012). Dynamic measurement of pennation angle of gastrocnemius muscles during contractions based on ultrasound imaging. *Biomed. Eng. Online* **11**, 63. doi:10.1186/1475-925X-11-63

Zhou, G.-Q., Chan, P. and Zheng, Y.-P. (2015). Automatic measurement of pennation angle and fascicle length of gastrocnemius muscles using real-time ultrasound imaging. *Ultrasonics* **57**, 72-83. doi:10.1016/j.ultras.2014.10.020